東京大学 大学院新領域創成科学研究科
基盤科学研究系
先端エネルギー工学専攻

平成 21 年度

修士論文

Application of microwave beam control technology

to a Microwave Rocket

－　マイクロ波ビーム制御技術のマイクロ波ロケットへの応用　－

2010 年 2 月提出
指導教員　小紫　公也　教授

086080　山口　敏和

Acknowledgements

Contents

1. Introduction

Microwave Rocket

Microwave Rocket is one of the Beamed Energy Propulsion systems applicable to future space launches. Propulsive energy is repetitively supplied by pulsed microwave beams irradiated form the ground and the atmospheric air is used as a propellant, so that it can be propelled without any energy sources or propellants onboard. In addition, it does not require complicated structures like combustion chambers and turbo pump systems equipped on conventional liquid rocket engines. Therefore, it is expected to achieve a high payload ratio and a low launch cost.[1, 2]
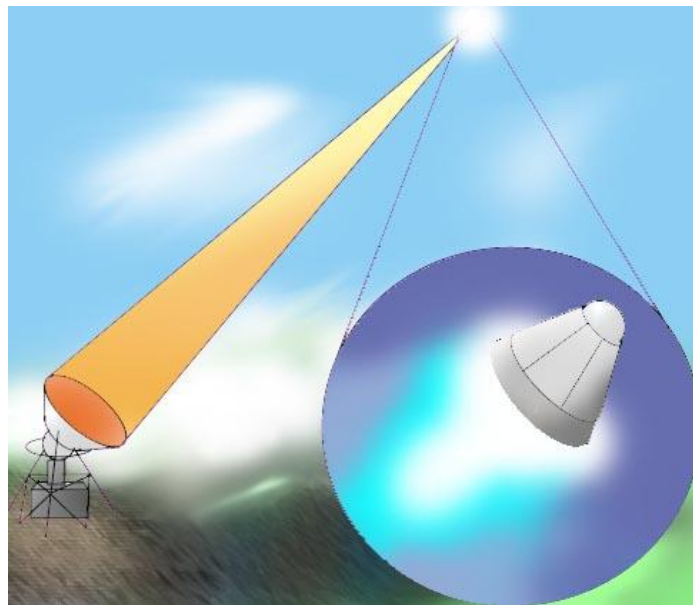

Figure 1-1. Schematic figure of Microwave Propulsion.

Although the construction cost of high-power beam source stations would be expensive, the cost per one launch can be decreased with the multiple launches in the order of a hundred to a thousand. Moreover, compared with laser generators, microwave

generators have been already developed higher power and less expensive, and a microwave beam can be combined with other beams by a phased-array technology in order to construct a GW-class beam for future launches.

Microwave Rocket consists of a cylindrical tube and a reflector for ignition. The closed end of the cylindrical tube has a conical reflector called "a thrust wall" and the other end is an inlet of the microwave beam, in which air is exhausted and refilled through. Its thrust generation mechanism is explained in the analogy of the pulse detonation engine (PDE) model, which is based on propagation of the detonation wave in a tube shaped engine, as shown in Fig. 1-2. A detonation wave starts from the tube end and propagates in the tube towards the exit at a constant velocity. A rarefaction wave follows the detonation wave, but the pressure in the tube is still higher than atmospheric pressure. Pressure at the thrust wall is constant during three steps: the shock wave leaving the closed tube end, pressurized air in the tube exhausted, and an expansion wave coming back from the end to the thrust wall. After that, pressure in the tube gradually decreases to the atmospheric pressure while oscillating.[3, 4] By a repetition of this cycle, thrust is generated one after another. The thrust impulse can be estimated by integrating the pressure history at the thrust wall. In the Microwave Rocket, microwave plasma heated efficiently converts the microwave energy to the kinetic energy of the driving gas, instead of using chemical reactions.

In our previous experiments, the momentum coupling coefficient C_m, which is a ratio of thrust impulse to input microwave energy, recorded about 400Ns/MJ by a single-pulse irradiation at atmospheric pressure, though it decreased with the pulse repetition rate in multi-pulse operation.[5] This is because the air refill is not completed in the short pulse intervals and the heated gas remains in the tube. This thrust degradation was recovered using a forced air-breathing system, simulating air intake at the supersonic flight.[6]
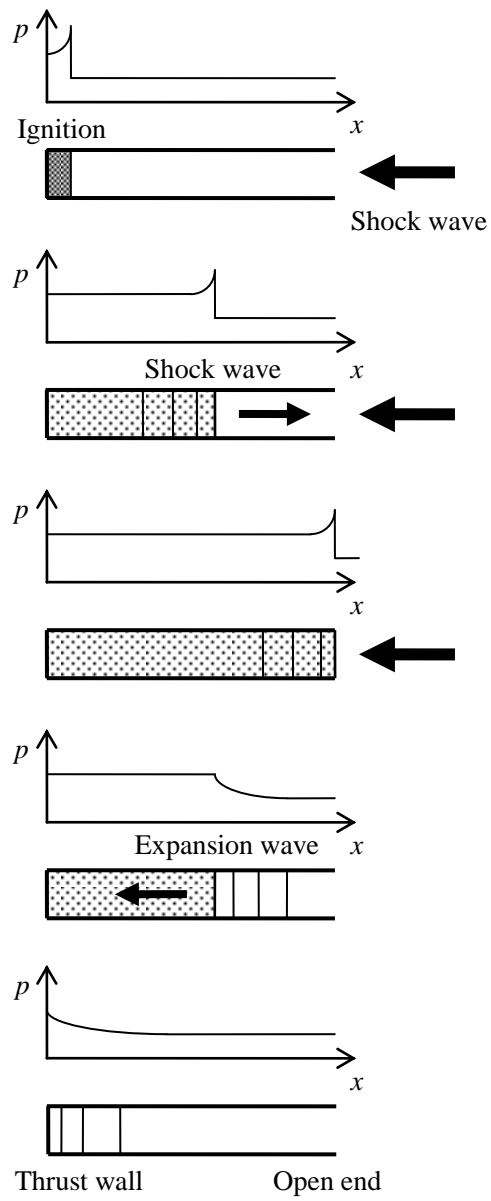
Figure 1-2.   Thrust generation model of a pulse detonation engine.

Gyrotron

A 1MW-class 170GHz gyrotron was used as a microwave generator. It was developed at Japan Atomic Energy Agency (JAEA) for Electron Cyclotron Heating and Current Drive (ECH&CD) in International Thermonuclear Experimental Reactor (ITER).[7] Its specifications are listed in Table 1. It has achieved 60% energy conversion efficiency from electricity with Single-stage Depressed Collector (SDC) as an energy recovery system.[8] The millimeter wave was transmitted through corrugated waveguides, and the profile of the output millimeter wave beam was a fundamental Gaussian beam with 20.4mm radial beam waist.

Table 1.　Specifications of the JAEA's gyroton.

Parameters	Values
Microwave Frequency	170GHz
Output Power	< 1MW
Pulse Duration	0.1ms to 1000s
Beam Profile	Gaussian
Beam Diameter	40mm
Electrical Efficiency	50-60%

FIGURE 1-3.   Gyrotron.
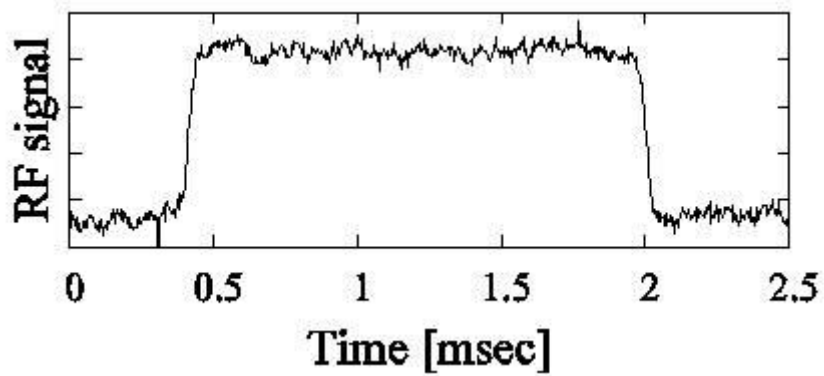
FIGURE 1-4.   History of microwave pulse.

2. Experiments

2-1) Long-range beam transmission

Objective

The directionality of microwave is much worse than that of laser, however, millimeter wave band of microwave can be achieve the quality of the directionality for BEP use. Consider the following equation which describes the Gaussian beam wave propagation under consideration of diffractions.

$$w(z) = w_0 \sqrt{1 + \left(\frac{z}{z_0}\right)^2}$$

$$w_0 = \sqrt{\frac{2z_0}{k_0 n}}$$

(2-1-1)

$w(z)$: spot size at propagation distance of z

w_0 : Beam waist (radius)

z_0 : Rayleigh range

k_0 : wave number in vacuum

n : refraction index

According to this equation, when the beam waist is wide enough, millimeter wave can have a good directionality. For example, if we never consider other matters such as transmittance of vapor or atmosphere, 370GHz millimeter wave with 15m beam waist diameter is only diffused 10% under 100km beam transmission. It would be possible to launch vehicles into LEO by acceleration from 0km to 100km altitude [1]. Actually when we think of "Microwave Rocket launch of 100kg-order vehicle by 0.1-1GW powered beam," the problem caused by the increment of transmitted power is some environmental influence because of the high power density.

In order to get some information if the long-range energy transmission by high power microwave beam is really hopeful or not, an experiment with this beam control technology was considered. Since the output beam diameter from the gyrotron was not easy to change, the diameter of the beam should be expanded by some device as shown in Fig.2-1-1. Moreover, the transmitted beam should be narrowly collimated in order to get the high power density beam as the original one, because low power density beam couldn't achieve high thrust performance in former studies.
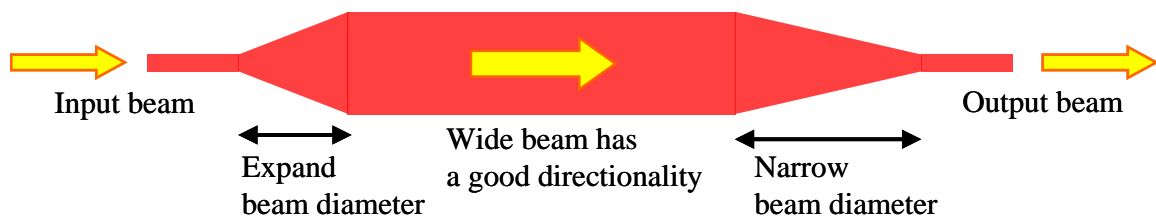
FIGURE 2-1-1.   Beam is expanded and narrowed for long-range power transmission.

Experimental setup

To achieve a long-range microwave power transmission, the beam diameter was expanded to 6 times wider by using a set of parabolic mirrors on the transmitter side, and narrowed to the same scale as original on the thruster side as well. Figures 2-1-3, 4 show the schematic of this system, the designed beam road and the pictures. Microwave was generated by 170GHz gyrotron at JAEA with high repetition pulses of around 100Hz and 400kW, and its original beam waist radius was 20mm from the transmission through the corrugated waveguide and the sapphire window. If the original 20mm beam is used for transmission, the beam size will be diffused to about 3 times larger after 2m transmission. The beam sized to 120mm can be transmitted with less than 10% (actually designed to 7.3%) of diffusion after 10m beam transmission according to the Equation 2-1-1.
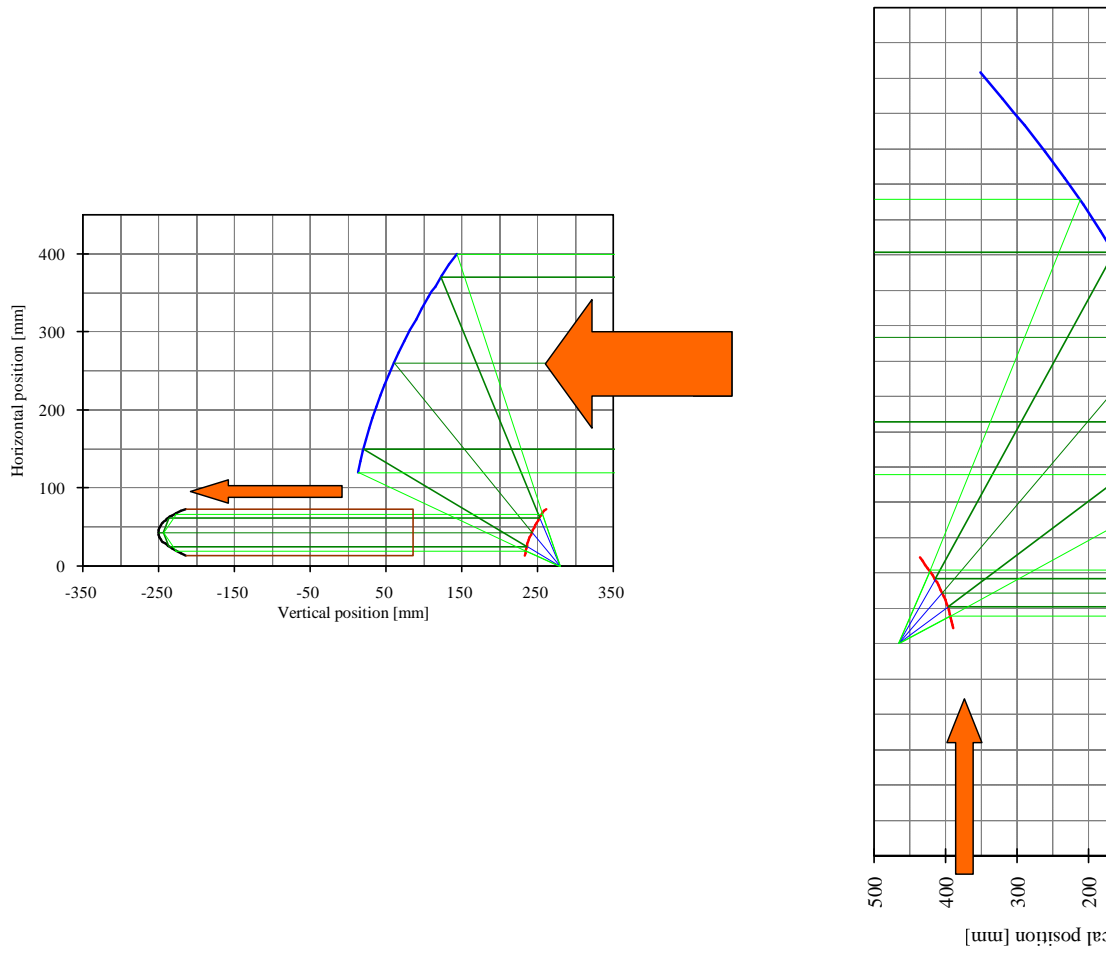
FIGURE 2-1-2.   Schematic of long-range beam transmission system and the beam road.

FIGURE 2-1-3.   Pictures of the long-range beam transmission system.
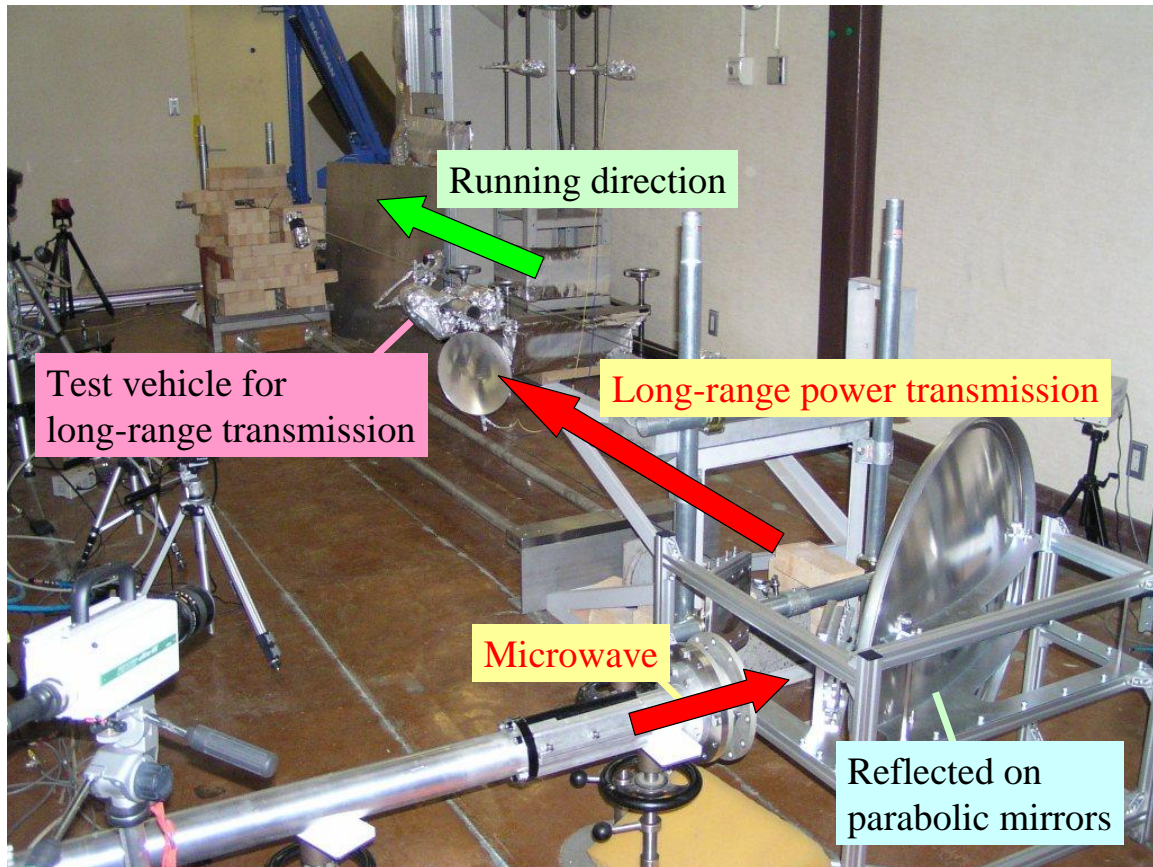
FIGURE 2-1-4.   Overhead view picture of the long-range beam transmission system.

Test vehicles shown in Fig. 2-1-5 were running on guide wires against a little friction. Two types of vehicles were prepared to get high thrust performance. One is called "Type B" weighed 1kg, and it was with various length of metallic tubes without any air-flow system. The other is called "Type C" weighed 2kg, and it was with a 500mm metallic tube with an on-board air-flow system. The tube length L of the Type B vehicles was changed from 200mm to 500mm in order to obtain the optimum tube length dependent on the pulse repetition frequency. The pulse repetition frequency f was changed from 20Hz to 200Hz.

Generated thrust was measured by using laser displacement meter as shown in Fig. 2-1-6. The signal from the meter is proportional to the displacement in the range of 0.5m, and the thrust was calculated from the displacement history.

FIGURE 2-1-5. Test vehicles for long-range transmission. (Top : Type B, bottom : Type C)

FIGURE 2-1-6.   Thrust measurement system by using laser displacement meter.

Results and discussions

Results showed that transmitted power heated the screen sheet as shown in Fig. 2-1-7, and atmospheric breakdown successfully occurred in the range from 1m to 5m.

1m point →

3m point →

5m point →

IR images on screen sheet

Breakdown pictures at each distance
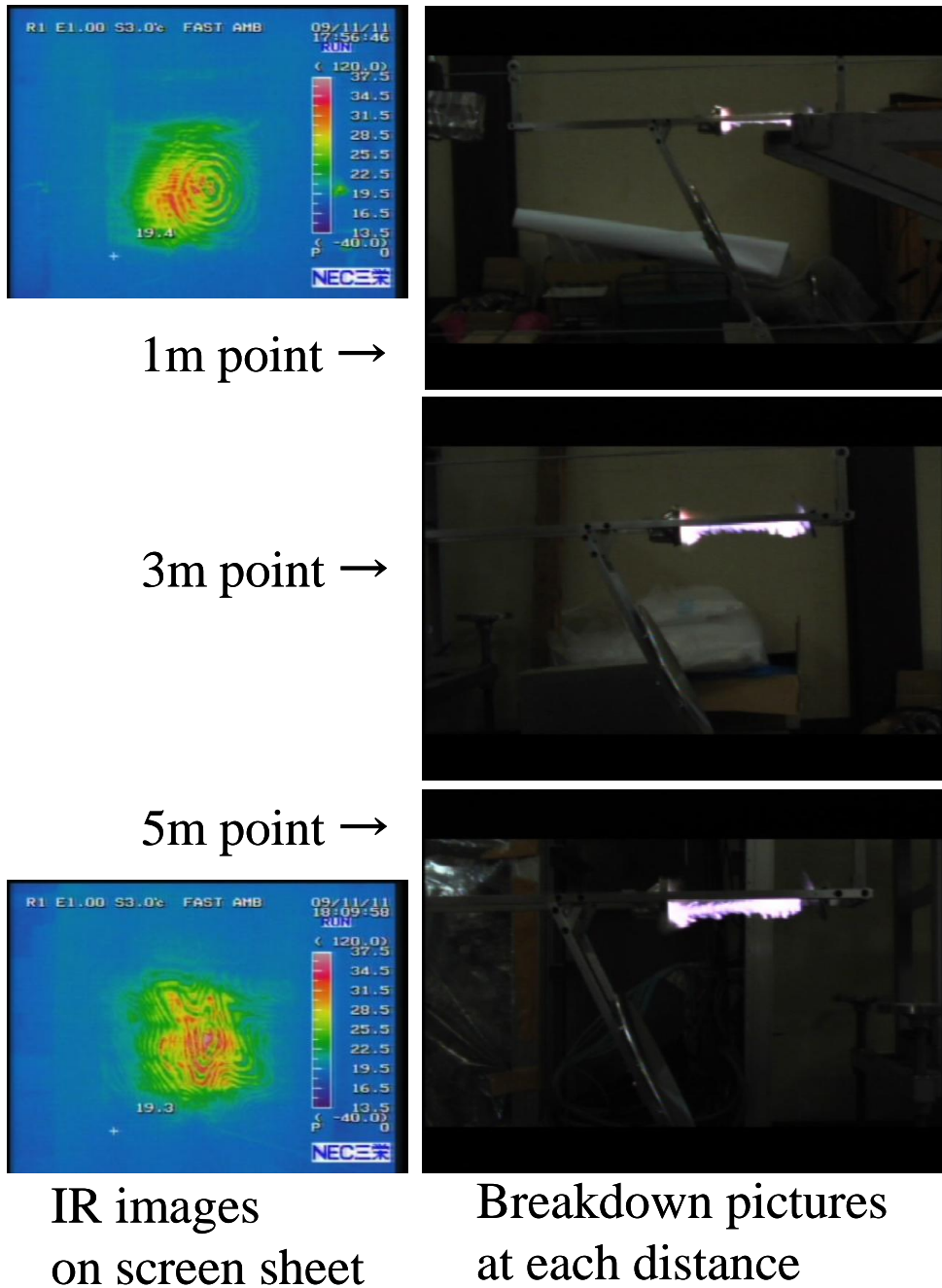
FIGURE 2-1-7.   IR images and breakdown pictures at each distance.

Figure 2-1-8 shows that the result of laser displacement measurement and the microwave pulse input history. Results showed that thrust was continuously generated after long-range beam transmission.
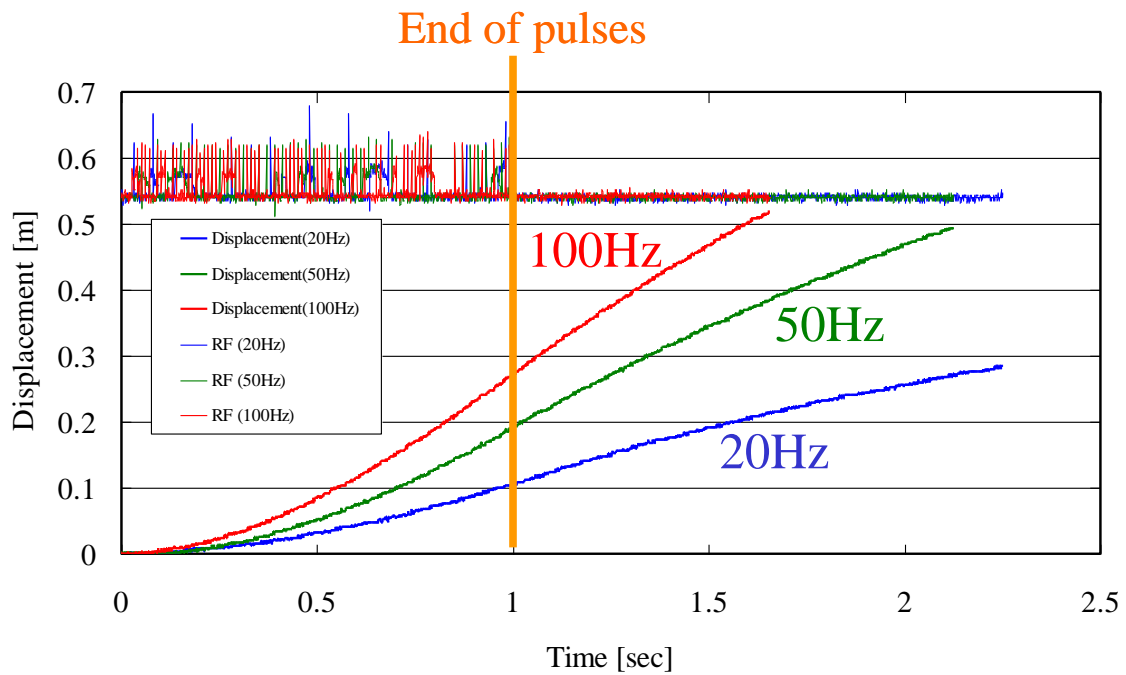
FIGURE 2-1-8.   Laser displacement measurement at 2m distance from the transmitter.
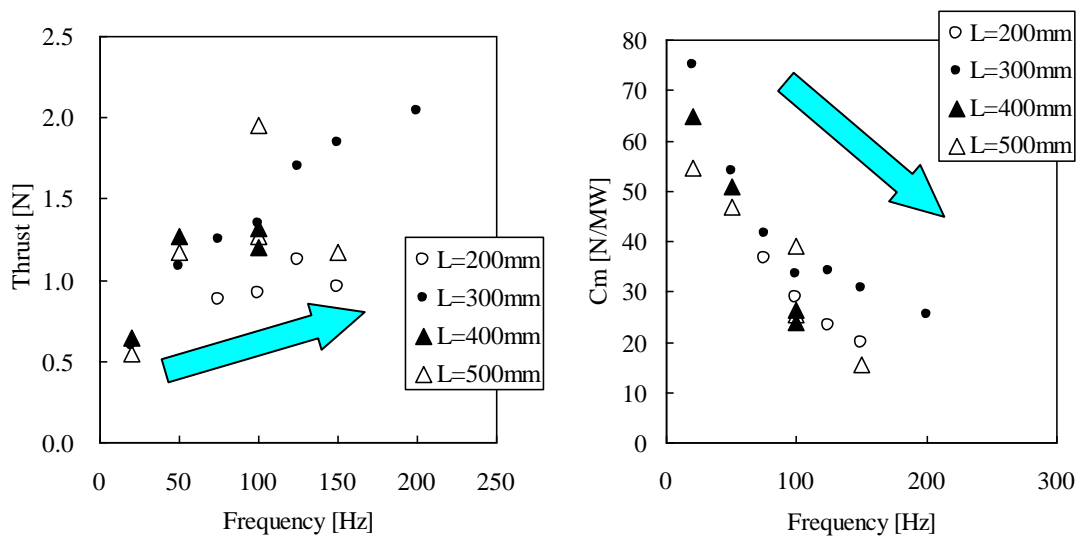
FIGURE 2-1-9.   Thrust and C_m dependence on the pulse repetition frequency and the tube length.

Figure 2-1-9 shows the measured thrust and C_m. Thrust increases with pulse repetition frequency, while C_m decreased. There was not so strong dependence of C_m on the tube length, even the longer tube length improved the thrust as shown in Fig. 2-1-10. Type C vehicles improved the thrust by using the on-board air-flow system as shown in Fig. 2-1-11.
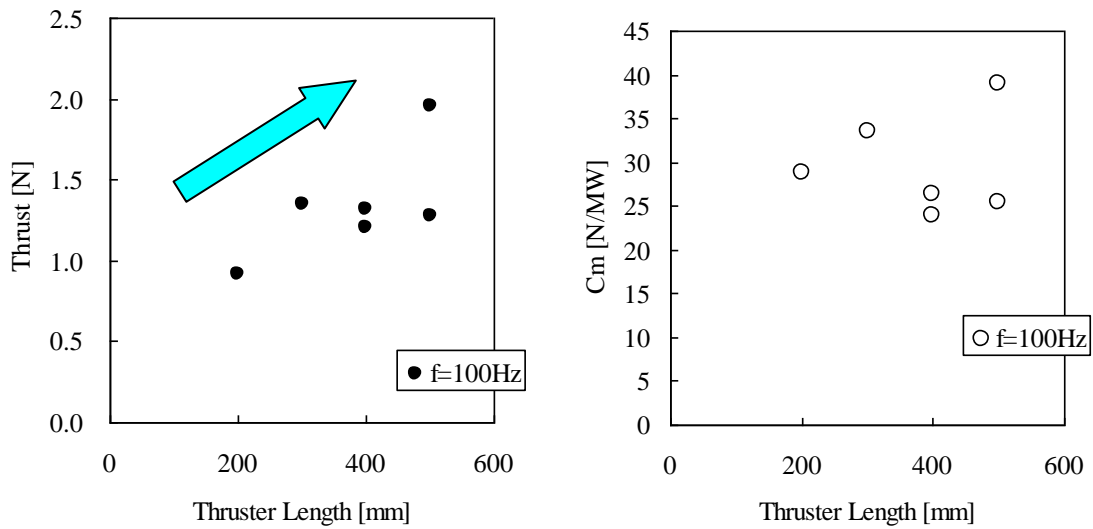
FIGURE 2-1-10.   Thrust and C_m dependence on the tube length at f=100Hz.
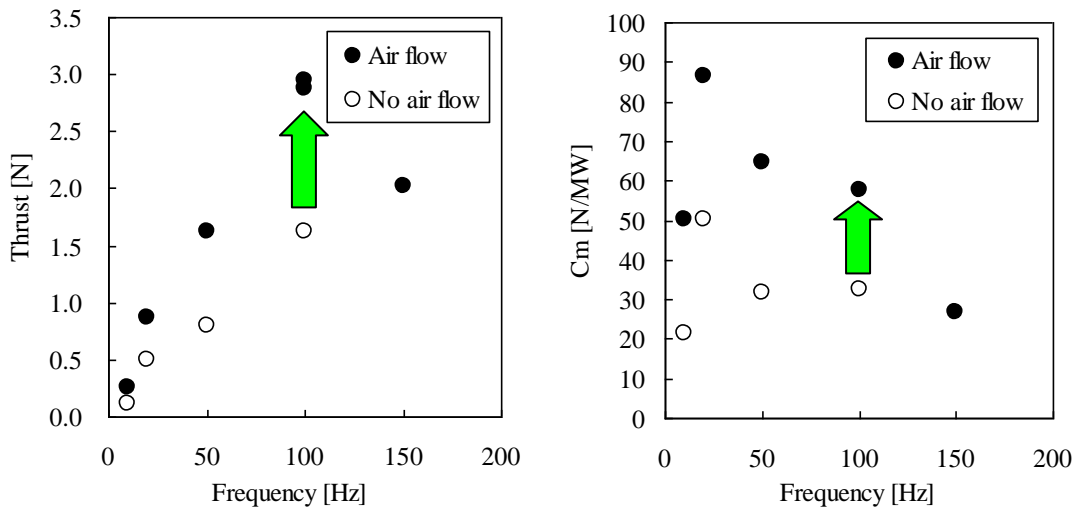
FIGURE 2-1-11.   Thrust and C_m improvement caused by air-flow system on the Type C vehicle.

Conclusions

The long-range beam transmission system was successfully worked and thrust was generated after the meter-range transmission. Thrust and C_m were calculated by using laser displacement measurement. The results of thrust and C_m had dependences on the tube length and pulse repetition frequency, and well agreed with the previous studies of Microwave Rocket, even the C_m was still less than that of expected.

Next steps

This long-range transmission technology also implies the possibility of high-power wireless transmission for future applications including rocket propulsion.

Although the thrust dependences on the tube length and the pulse repetition frequency were not in precise discussion because of the lack of the data in the graphics, the thrust mass ratio is still much less than 1 for vertical launch. The C_m was also still less than the potential value, thus there are some ways to improve the thrust, such as with a higher air-flow system, a multi-head type vehicle. The kg-order vehicle's m-order flight and hovering would be a next possible target in several years.

2-2) Beam profile transformation

(From Gaussian profile to Ring, Flat-top profile)

Objective

In past studies, the Gaussian profile beam was the only beam that can be supplied, however, the profile will be transformed in future practical use of Microwave Rocket, because this flexibility of microwave is one of advantages of microwave against laser and the flexibility can make new effective thruster shape accepted as a vehicle. In addition, the atmospheric breakdown caused by millimeter wave showed a filament structure as shown in Fig. 2-2-1. As represented by this phenomenon, atmospheric breakdown has an interesting point of view and another beam profile with other distribution of the local power density has some possibilities to change the filament structure.
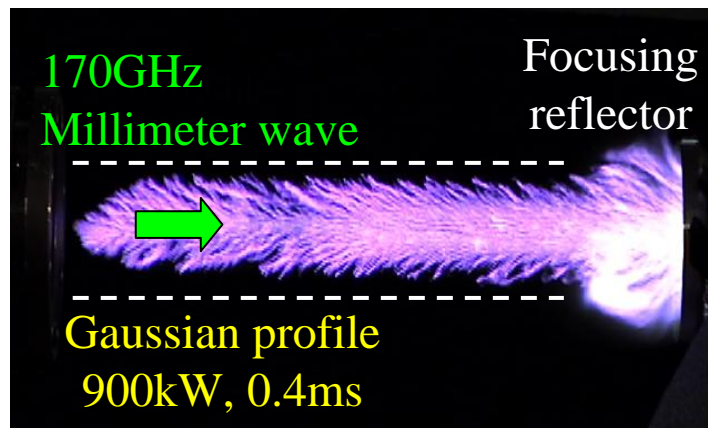
FIGURE 2-2-1.   Plasma propagation with a filament structure.

Experimental setup

Therefore the Gaussian profile beam was transformed into the following two beams with other profiles; one is Ring profile and the other is Flat-top profile. These

transformations were caused by the reflection between a pair of mirrors which has microscopic asperities on its surface. The mirrors are called "phase correcting mirror." Figure 2-2-2 shows the experimental results of the low power performance of the phase correcting mirror system. The mirrors were well working.
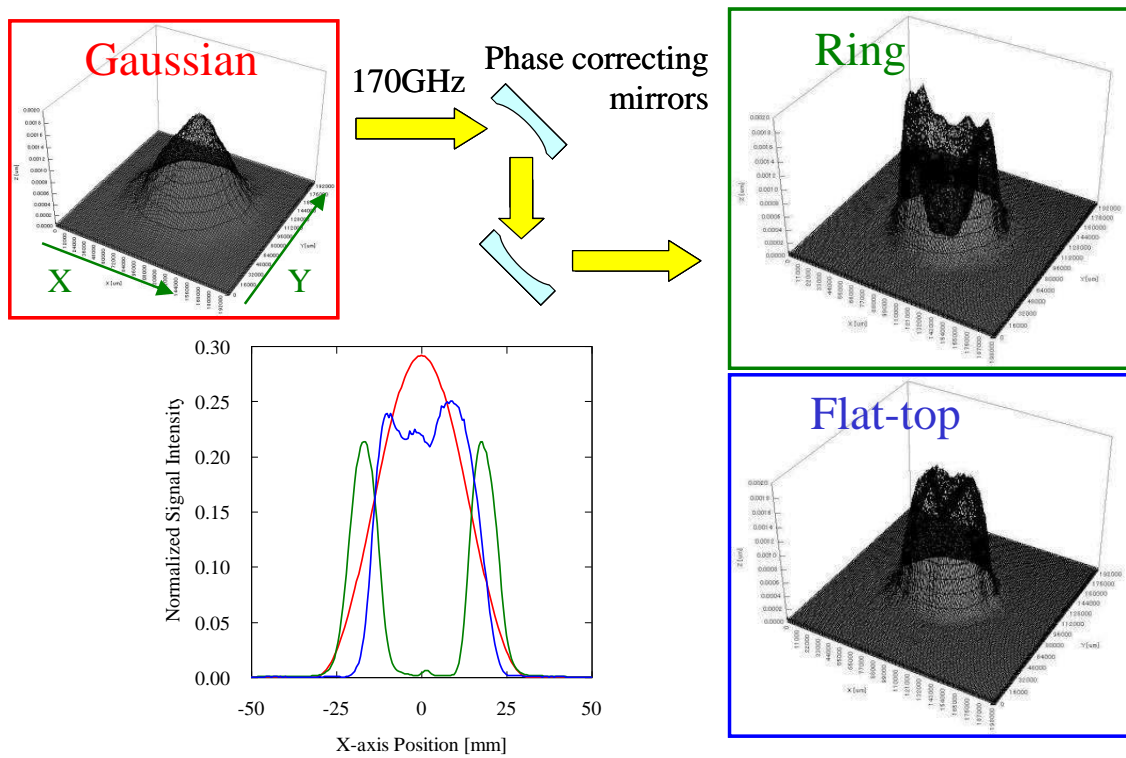
FIGURE 2-2-2.   Low power performance of the phase correcting mirror system.
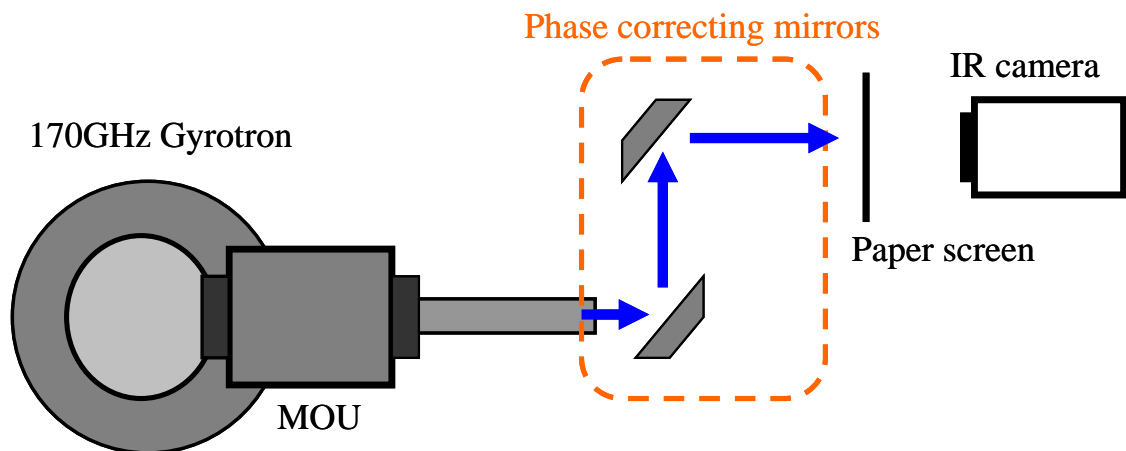
FIGURE 2-2-3.   Schematic of the beam profile transformation system.
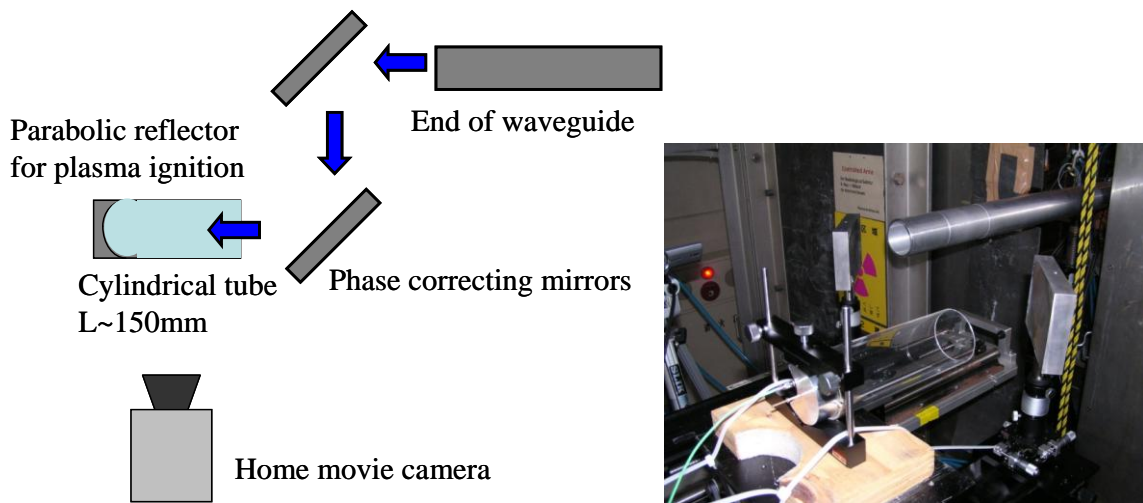
FIGURE 2-2-4.   Schematic of plasma observation system.

Figure 2-2-3 shows the schematic of the system with high power microwave generated by 170GHz gyrotron. Figure 2-2-4 shows the plasma observation system.

Results and discussions

Figure 2-2-5 shows the results of IR images compared with the designed distributions and the images of the plasma propagations caused by the different beam profiles were shown in Fig. 2-2-6. The input power of microwave was 200kW and velocities of the ionization fronts were measured by the home movie camera with changing the microwave pulse duration.
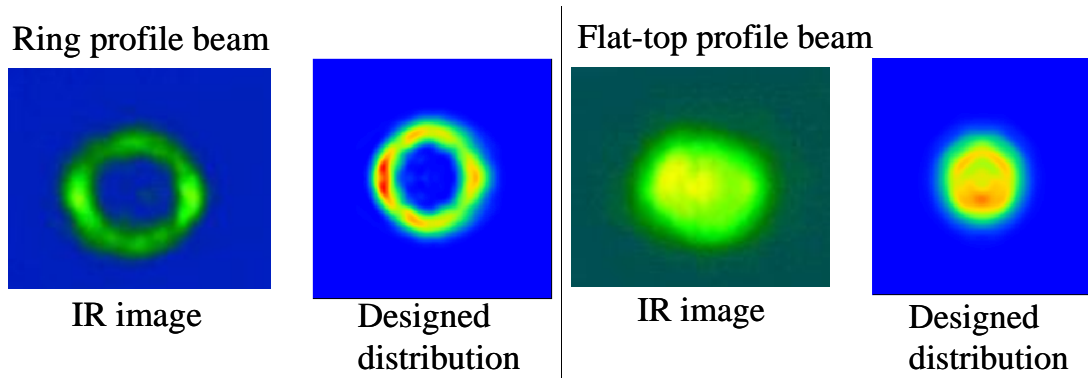
FIGURE 2-2-5.   IR images and designed distributions.

Input microwave power : 200kW

Ring beam

Gaussian beam

$S_{peak} = 33$ kW/cm^2
$U_{ioniz} = 140$ m/s
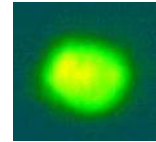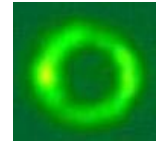
Flat-top beam
$S_{peak} = 16$ kW/cm^2
$U_{ioniz} = 68$ m/s

FIGURE 2-2-6.   Propagating plasma powered by the transformed beam.

Conclusions

The beam profile was transformed from Gaussian into Ring or Flat-top by using the phase correcting mirror system. The shape of the propagating plasma was dependent on the difference of the beam profile, although the dependency was not so strong in this experimental condition. The structure was changed to no-center shape plasma in case of the Ring beam, and it was changed to wider plasma shape in case of the Flat-top beam. The propagating structure of the plasma was indicated to be leaded by the gradient of the local power densities, and higher local power density leaded faster propagation. Moreover, the propagating velocity of the ionization front would be dependent on the peak value of the local power density supplied by the microwave beam.

Next steps

To be sure on what the propagating structures of the plasma is strongly dependent,

observation of the plasma propagation by a fast-framing camera is needed as a next step.

One goal of this application of the beam control technology is to control the plasma shape.

2-3) Visualization of the shock wave around the focal point

Objective

In this section, a microwave parabolic thruster was considered, and the cycle of thrust generation processes is shown in Fig. 2-3-1, as the following four steps: 1) A high-power microwave beam is focused in air by a parabolic mirror and a breakdown occurs. 2) The breakdown plasma is heated by absorption of following microwave beam energy, and generates a next ionization region on the beam direction. At the same time of the ionization region propagation, it drives a blast wave generated by the breakdown. 3) The blast wave which leads high pressure behind imparts thrust to a focusing mirror, which also works as a thrust wall. 4) Finally, air is refilled into the thruster. A steady thrust consists of the repetition of these processes.
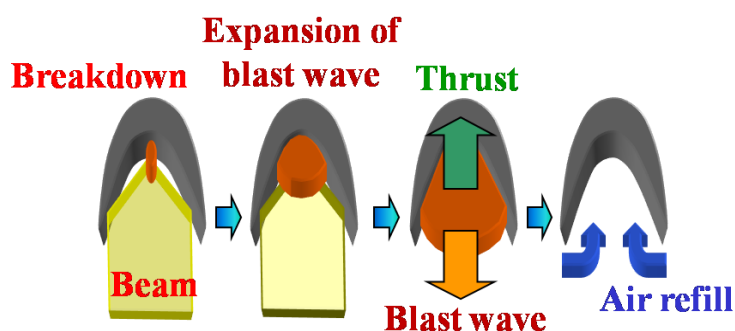
Figure 2-3-1. Thrust generation process.

The thruster has a simple parabolic mirror, and the mirror also has a roll to impart a thrust impulse from a high pressure wave driven by microwave plasma, thus the shape of

the mirror is a key of the thruster design. In previous studies, the propagation structure of millimeter wave plasma was observed [3], however, there was no image showing the structure of relationships between shock waves and plasma. Thus shock wave driven by microwave plasma was visualized at the area around the focal point. This is important for a discussion of physical structures related to the energy conversion processes from a microwave to plasma, and from plasma to a blast wave.

In previous studies, the propagation velocities of the ionization front of millimeter wave plasma and a shock wave were measured using 170GHz high-power gyrotron. The propagation velocity of the ionization front became supersonic when power density was greater than 75kW/cm^2. Propagating plasma front produces compression waves which were combined and formed a normal shock wave in front of the ionization front. When the ionization front propagates in supersonic, the shock wave and the ionization front have nearly same velocity. Oda *et al.* presented a one-dimensional propagation model of the shock wave driven by microwave plasma which is the combination of a normal shock wave and propagating plasma front. Although the shock wave and the ionization front have the identical velocity, its propagating model was similar to slow combustion in a tube [4].

Shock wave driven by laser plasma shows a different structure which resembles a detonation wave. In the case of a Laser Propulsion system, a high-power pulse laser generates high power density experiments, and two propagating structures were observed. During high power densities, at several MW/cm^2 level, plasma and a shock wave attached and propagated together. This structure is called Laser Supported Detonation (LSD) structure. On the other hand, with the decrease of laser power density, the plasma and shockwave detached and propagated separately at a certain power density condition, and this structure is called Laser Supported Combustion (LSC) structure. Transition from LSD

to LSC was defined as the termination of LSD. The termination condition of LSD is an important point to enhance thrust performance of the Laser Propulsion system, and it was experimentally observed [5].

In previous computational studies on Microwave Propulsion, two structures similar to LSD and LSC were predicted in a one-dimensional propagation model. At high microwave power densities, the structure was defined as Microwave Supported Detonation (MSD), and for lower power densities, Microwave Supported Combustion (MSC). The currently used gyrotron could not produce a high power enough to generate the MSD structure, thus experimental visualizations were done only for MSC.

However, by focusing the microwave, the microwave power density could raise to a level to produce a MSD structure. Therefore, by visualizing the initiation of the microwave plasma at the focal point, we could observe the MSD structure. Moreover, at the focal area, distance from the focal point makes the local power density decrease, thus the transition from high power density phenomenon to low power density one, from MSD to MSC, is able to be observed.

Experimental setup

A 1MW-class 170GHz gyrotron was used as a microwave generator. A 3-dimensional parabolic mirror was used in order to generate a thrust impulse on its face. Thus the face shape of the mirror has a roll of thrust generation. The mirror was made of aluminum, its diameter was 55mm, and its focal length was 22.32mm from the center point on its face.

Shock waves were visualized by a shadowgraph method as shown in Fig. 2-3-2. A He-Ne laser, the wavelength of which was 633nm, was used as a light source, and photo images were taken by a fast framing camera, Ultra-8 made by nac Image Technology Inc..

In these ways, propagating velocities were measured and structures of shock waves and ionization fronts were observed. Here, an ionization front is the edge of the plasma region on a microwave irradiation beam line.
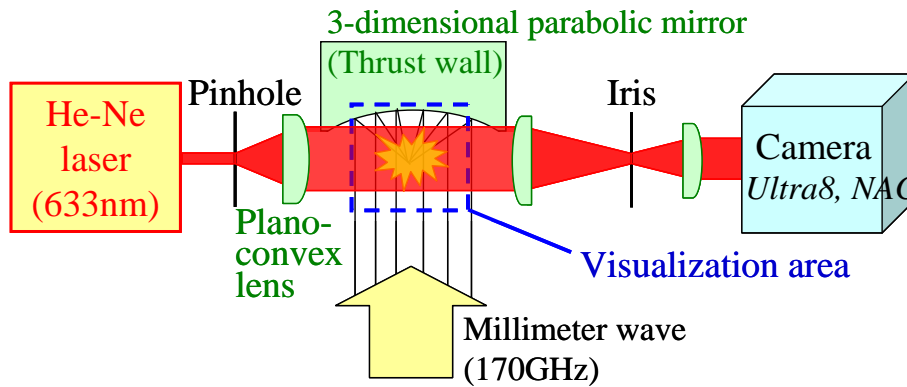
Figure 2-3-2. Schematic of a shadowgraph method.

Results and discussions

A shadowgraph method visualized the shock wave and the plasma region around the focal area. Figure 2-3-3 shows these images. The shape of the shock wave was not spherical, and these images include two important things. One is to get the information of any expanding directions, especially toward the parabolic reflector as a thrust wall. The other is to get the phenomena for higher local power density region than any previous studies. Positions of the shock front, the front on the axis of the shock wave, and the ionization front, the front of the plasma region, were measured.

For analysis, A-line and B-line were defined as shown in Fig. 2-3-4. B-line is the axis on the main beam. Microwave energy is absorbed by plasma on the B-line, but microwave is not screened outside the plasma region. The remained microwave reflects on the outer surface of the parabolic mirror, and it is focused along A-line. Therefore, plasma absorbs

the microwave energy and the shock wave can be driven by the plasma on both A-line and B-line. The shape of the shock wave is dependent on the structure of the heated plasma.
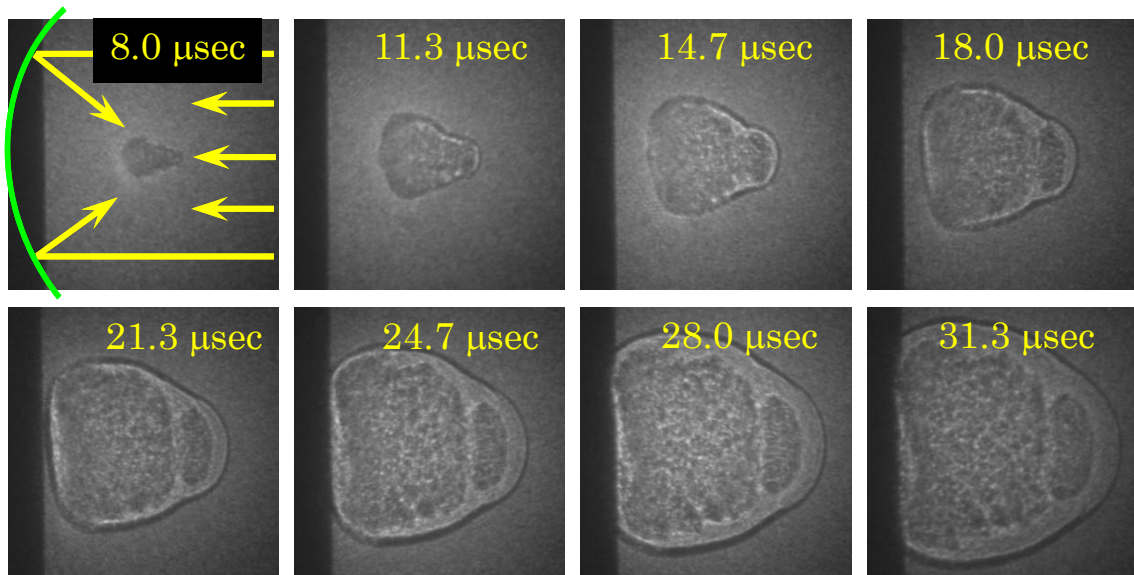
Figure 2-3-3. Shadowgraph images. (Shutter speed : 0.3 million frames/sec, Exposure time : 150 nsec, Gas : air, Pressure : 1atm, Incident microwave power : 598kW, Pulse duration : 0.5msec)
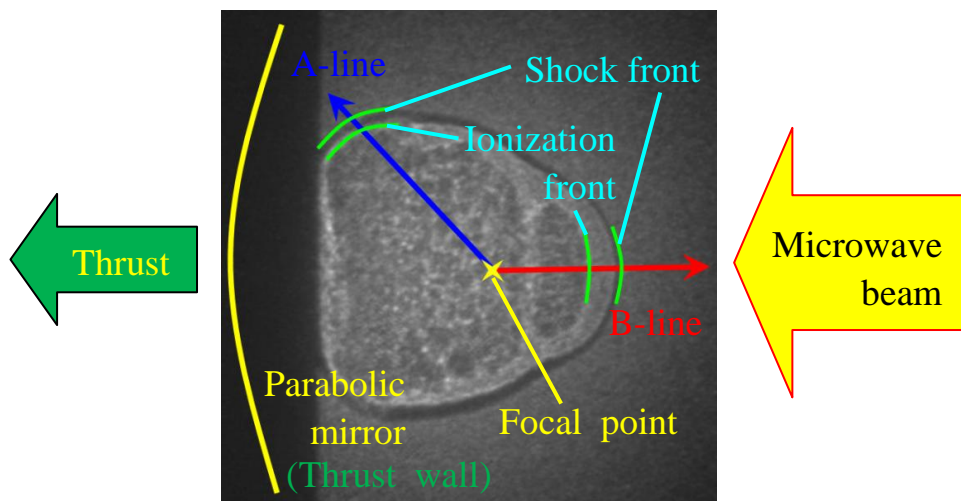
Figure 2-3-4. Propagation of millimeter wave plasma at the focal point and definitions of the analytical lines.

Along the A-line, the local power density at the propagating ionization front decreases with the increase of the distance from the focal point to the ionization front. On the other hand, the local power density on the B-line changes much less than that on the A-line, and is nearly constant.

Using these shadowgraph images, propagating shapes of shock front and ionization front at different times were analyzed on two lines. Images for one microwave pulse were not more than eight because of the camera specification, thus settings of a shutter speed, a delay time and an exposure time were adjusted and data of several pulses were united for analysis. Experimental conditions were a 598kW microwave beam irradiation with ambient atmospheric air. The pulse duration of the beam was about 0.2msec, but it was much longer than 30μsec of phenomena at the visualized focal area.

Figure 2-3-5 shows analytical results on the A-line. Figure 2-3-5(a) shows the distance from the focal point to the shock front and the ionization front. The zero point of the time was defined as the time to start of an RF signal, but delay times of breakdown were not stable to each pulse. Therefore, this horizontal axis was transformed into an offset time, and points on the graph were almost on the same curve. Figure 2-3-5(b) shows the propagation velocity under the distance from the focal point to the ionization front. In the same way, Fig. 2-3-6 shows results on the B-line.

Figure 2-3-5(a) indicates that there are two types of the structure between the shock wave and the plasma, first one is a shock wave with an ionization front, the other is a shock wave set apart from ionization front. But Fig. 2-3-6(a) only indicates the second type of the structure. This result showed that there was an MSD structure at the focal area on the A-line because the local power density was extremely high, on the other hand there was not such a structure on the B-line, and structures were an MSC structure. In an MSD structure, a shock wave and an ionization front can propagate with each other because the
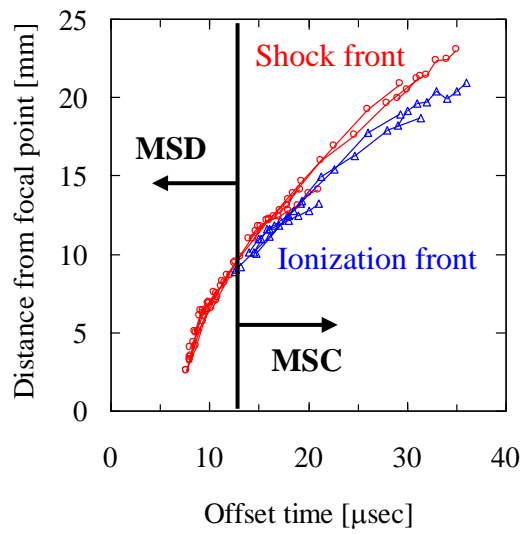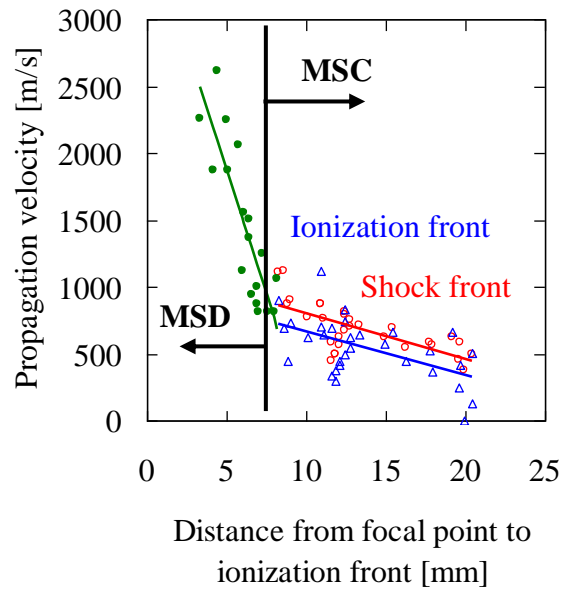
FIGURE 2-3-5. Results on the A-line. (a) Distance from the focal point of the shock front and the ionization front. (b) Propagation velocity under the distance from the focal point to the ionization front.
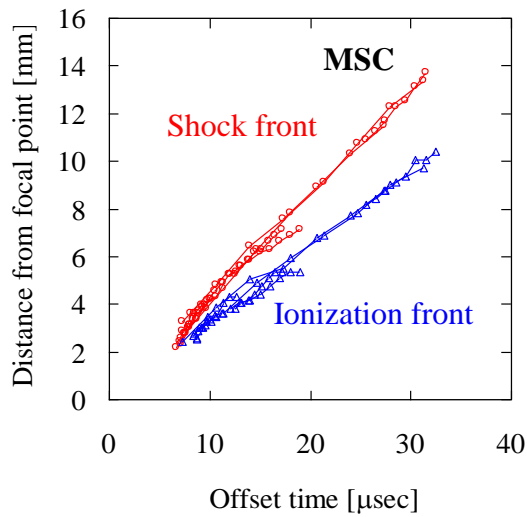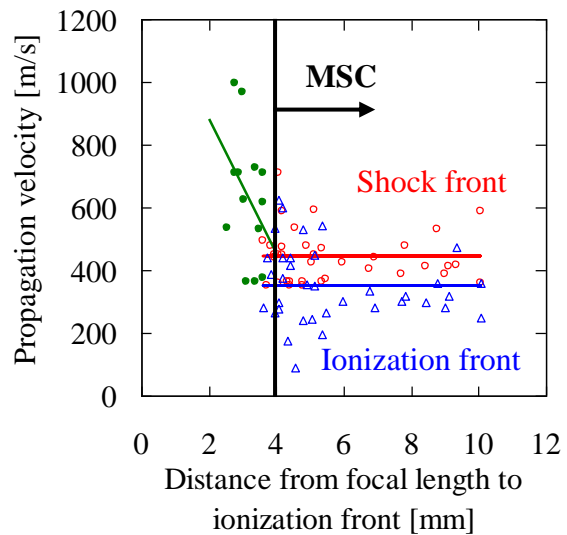

FIGURE 2-3-6. Results on the B-line. (a) Distance from the focal point of the shock front and the ionization front. (b) Propagation velocity under the distance from the focal point to the ionization front.
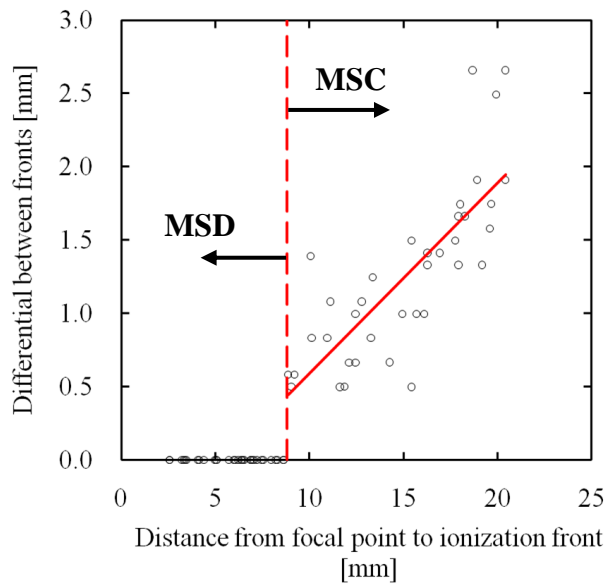
FIGURE 2-3-7. Differential between two fronts under the distance from the focal point to the ionization front on the A-line.

plasma can be heated or generated by the higher power density. On the other hand, in an MSC structure, a shock wave cannot propagate with an ionization front, although the shock wave is still driven by the ionization front.

Since the local power density change with position of the focal point, the horizontal axis in Fig. 2-3-5(b) is related to the local power density. When the ionization front draws apart the focal point, the local power density becomes lower. In this figure, the propagation velocity of the MSD structure near the focal point was more than 2,500m/s, and the velocity decreases when the distance increases. However, MSD transits to MSC at around 8mm from focal point, where the velocity was about 800m/s. Previous studies on one-dimensional numerical analysis implied the transition from MSC to MSD at a power density of 196kW/cm^2, where the velocity of the ionization front was 806m/s. Although the three-dimensional experimental results were discussed only by the local power density, both experimental and numerical results showed a good agreement.

On the other hand, the horizontal axis of Fig. 2-3-6(b) does not have such a property. The propagation velocity was fast near the focal point, but it was almost constant around 400m/s. This result was because the local power density along the B-line was almost same except for the area which is very near the focal point and has a high power density.

Figure 2-3-7 shows the differential between two fronts under the distance from the focal point to the ionization front on the A-line. At a certain distance, the differential suddenly started to grow up. The transition from MSD to MSC was produced at a certain local power density, where the distance from the focal point was about 8mm.

Conclusions

Shock waves driven by millimeter wave plasma were visualized at the focal area in a parabolic thruster. The propagating shape of the shock wave was not spherical, but dependent on the shape of the heated plasma front which absorbs a high-power microwave beam.

An MSD structure was observed on the focused microwave beam line as the one-dimensional numerical analysis on a higher local power density. In addition, the transition from MSD to MSC was observed at a certain local power density, and the propagation velocity of the shock front at the transition was about 800m/s. This result agrees well with the simulation assumed a one-dimensional propagating model.

2-4) Demonstration flight

(Vertical launch with repetitive pulse microwave beam)

Objective

The MW-class 170GHz gyrotron was recently improved to steadily generate repetitive pulse microwave beam. Therefore, a vertical launch of a light model rocket of Microwave Rocket has been done as a demonstration flight with high frequency multi-pulse operation.

Experimental setup

The microwave power was 600kW, the pulse repetition frequency was 100Hz, and the pulse duration was 1msec. Two model rockets were prepared as shown in Fig. 2-4-1. The left rocket of this figure is weighing 126g with a parabolic reflector for plasma ignition and has a taper metallic tube body; the top diameter was 56mm and the bottom diameter was 90mm. The right one is weighing 109g with a conical reflector and has an aluminum cylindrical body; the diameter was 100mm. The tube length of both rockets was 300mm.

FIGURE 2-4-1.　Light model rockets. (Left : 126g, right : 109g)
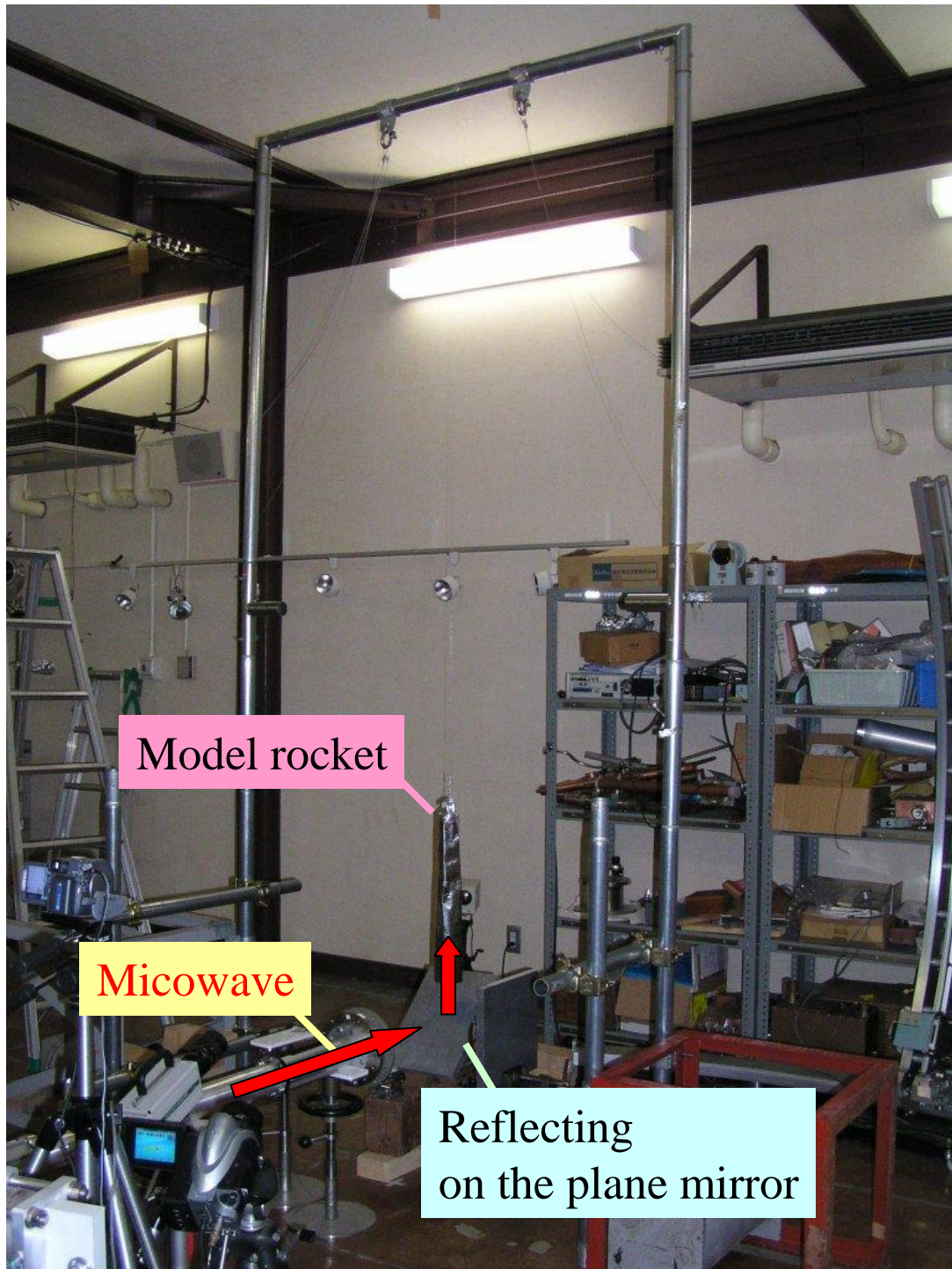
FIGURE 2-4-2.　　Setup of the launch experiment.

Figure 2-4-2 shows the setup of this experiment. The microwave was reflected on the aluminum plane mirror and go into the body of the model rockets.

Results

In the previous experiment in 2003, a plastic model rocket weighing 9.5g was launched at 2m altitude by a single-pulse microwave beam (930kW, 0.4msec). In this experiment, thrust was generated continuously for 1.2m vertical distance using a repetitively pulsed microwave beam (power : 600kW, pulse duration : 1msec, pulse repetition frequency : 100Hz) and the thrust was enough to lift up a metallic rocket weighing 126g which was one order of magnitude heavier than the previous model.
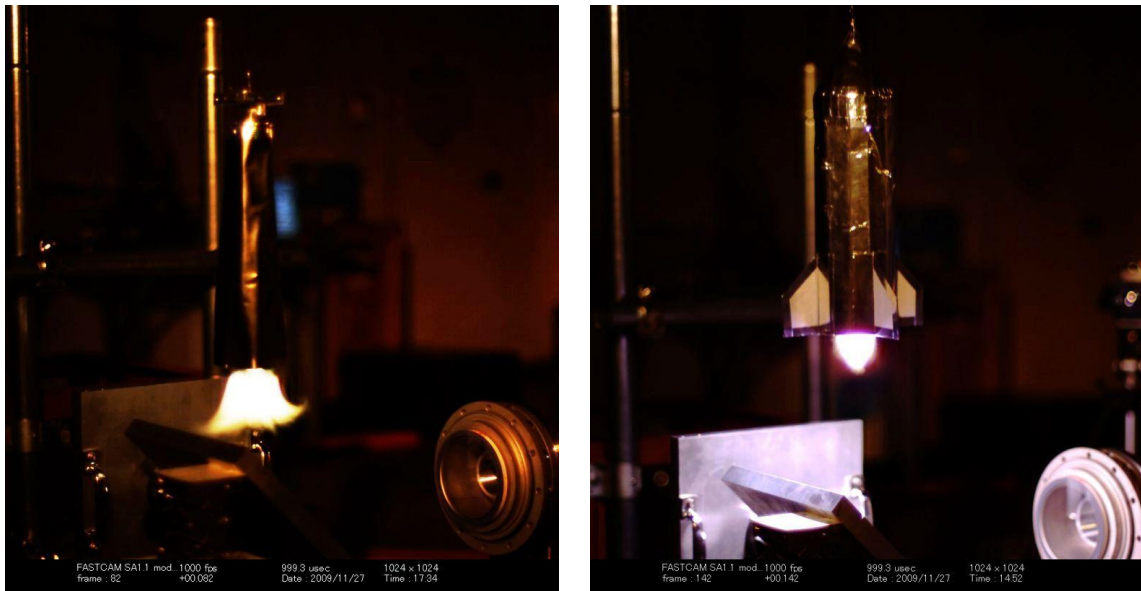
FIGURE 2-4-3.   Images taken by a fast-framing camera. (FASTCAM SA1.1, Photoron Ltd.)
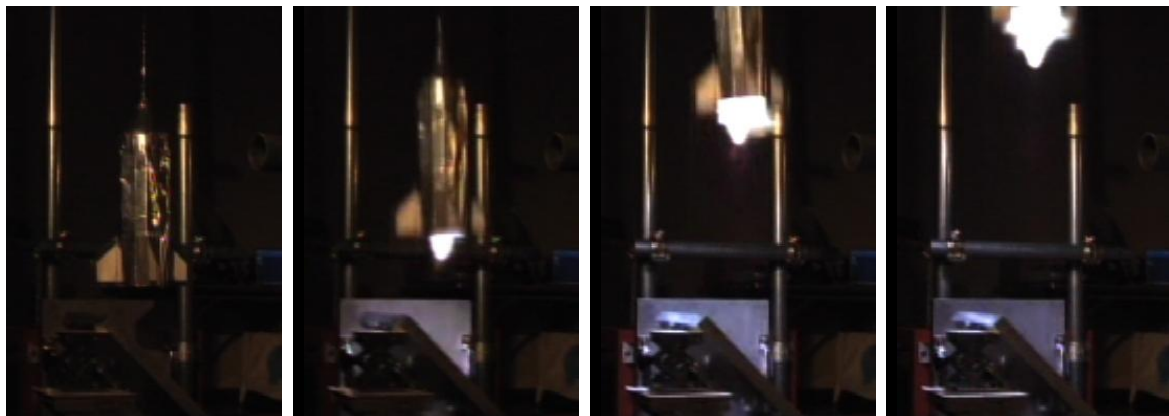
FIGURE 2-4-4.   Launch of the 109g model rocket. (1.2m flight)

FIGURE 2-4-5.   Launch of the 126g model rocket. (1.2m flight)

Next steps

Our future work is to launch a heavier rocket to a higher altitude by improving supplied power from a gyrotron and optical transmission systems, and by adding an air intake, and eventually, to launch 100kg payload into earth orbits.

3. Summary

3-1) Long-range beam transmission

The long-range beam transmission system was successfully worked and thrust was generated after the meter-range transmission. Thrust and C_m were calculated by using laser displacement measurement. The results of thrust and C_m had dependences on the tube length and pulse repetition frequency, and well agreed with the previous studies of Microwave Rocket, even the C_m was still less than that of expected.

2-2) Beam profile transformation

(From Gaussian profile to Ring, Flat-top profile)

The beam profile was transformed from Gaussian into Ring or Flat-top by using the phase correcting mirror system. The shape of the propagating plasma was dependent on the difference of the beam profile, although the dependency was not so strong in this experimental condition. The structure was changed to no-center shape plasma in case of the Ring beam, and it was changed to wider plasma shape in case of the Flat-top beam. The propagating structure of the plasma was indicated to be leaded by the gradient of the local power densities, and higher local power density leaded faster propagation. Moreover, the propagating velocity of the ionization front would be dependent on the peak value of the local power density supplied by the microwave beam.

2-3) Visualization of the shock wave around the focal point

Shock waves driven by millimeter wave plasma were visualized at the focal area in a parabolic thruster. The propagating shape of the shock wave was not spherical, but

dependent on the shape of the heated plasma front which absorbs a high-power microwave beam.

An MSD structure was observed on the focused microwave beam line as the one-dimensional numerical analysis on a higher local power density. In addition, the transition from MSD to MSC was observed at a certain local power density, and the propagation velocity of the shock front at the transition was about 800m/s. This result agrees well with the simulation assumed a one-dimensional propagating model.

2-4) Demonstration flight

(Vertical launch with repetitive pulse microwave beam)

In the previous experiment in 2003, a plastic model rocket weighing 9.5g was launched at 2m altitude by a single-pulse microwave beam (930kW, 0.4msec). In this experiment, thrust was generated continuously for 1.2m vertical distance using a repetitively pulsed microwave beam (power : 600kW, pulse duration : 1msec, pulse repetition frequency : 100Hz) and the thrust was enough to lift up a metallic rocket weighing 126g which was one order of magnitude heavier than the previous model.

Bibliography

1. Katsurayama, H., Komurasaki, K., and Y. Arakawa, "A Preliminary Study of Laser powered Launcher Performance," *Acta Astronautica*, Vol. 65, (2009), pp. 1032-1041.

2. Myrabo, L. N., "World record flights of beamed-riding rocket light craft," AIAA Paper 2001-3798, (2001).

3. Bussing, T., Pappas, G., "An Introduction to Pulse Detonation Engines," AIAA Paper 94-0263, (1994).

4. Endo, T., Kasahara, J., Matsuo, A., Inaba, K., Sato, S., and Fujiwara, T., "Pressure History at the Thrust Wall of Simplified Pulse Detonation Engine," *AIAA Journal*, Vol. 42, No. 9, 2004, pp. 1921-1930.

5. Y. Oda, K. Komurasaki, K. Takahashi, A. Kasugai, and K. Sakamoto, "Plasma generation using high-power millimeter wave beam and its application for thrust generation," *Journal of Applied Physics*, Vol.100, 2006, p.113308.

6. Oda, Y., Shibata, T., Komurasaki, K., Takahashi, K., Kasugai, A., and Sakamoto, K., "Thrust Performance of Microwave Rocket under Repetitive Pulse Operation," *Journal of Propulsion and Power*, Vol. 25, No. 1 (2009), pp.118-122.

7. Sakamoto, K., Kasugai, A., Takahashi, K., Minami, R., Kobayashi, N., and Kajiwara, K., "Achievement of robust high-efficiency 1MW oscillation in the hard-self-excitation region by a 170GHz continuous-wave gyrotron," *Nature Physics*, Vol. 3, No. 6, 2007, pp.411-414.

8. Kasugai, A., Sakamoto, K., Minami, R., Takahashi, K., and Imai, T., "Study of millimeter wave high-power gyrotron for long pulse operation," *Nuclear Instruments and Methods in Physics Research A*, 528, pp110-114, (2004).

9. Y. Oda, "Application of Atmospheric Millimeter Wave Plasma to Rocket Propulsion", Doctoral Thesis, The University of Tokyo, 2008.

10. M. Ushio, K. Komurasaki and Y. Arakawa, "Effect of laser supported detonation wave confinement on termination conditions", *Shock Waves*, Vol. 18, 2008, pp. 155-157.

学会誌掲載等

和文学術誌（査読有，掲載済）

[1] 山口敏和、畑井啓吾、小紫公也、荒川義博、「レーザー支持爆轟の終了条件とレーザー波長」、『プラズマ応用科学』、プラズマ応用科学会、16 巻 2 号、pp125－130、2008

欧文学術誌（査読有，投稿中）

[2] **Toshikazu Yamaguchi**, Yuya Shiraishi, Kimiya Komurasaki, Yasuhisa Oda, Ken Kajiwara, Koji Takahashi, Atsushi Kasugai, Keishi Sakamoto, "Microwave Rocket thrust performance for various microwave power densities and ambient pressures", 'Daejeon Conference Paper', Acta Astronautica.

学会発表等

国際会議での発表（自身で発表したもの．第一著者４件，第二著者１件）

[3] ***Yamaguchi T**, "Laser Supported Detonation Generated by a Solid Laser", '27th International Symposium on Space Technology and Science', 2009-b-32s, Tsukuba, Japan.(Jul.2009)

[4] ***Yamaguchi T**, Shiraishi Y, Komurasaki K, Oda Y, Kajiwara K, Takahashi K, Kasugai A, Sakamoto K, "THRUST DEPENDENCY OF THE MICROWAVE ROCKET ON MICROWAVE POWER DENSITY AND AMBIENT PRESSURE", '60th International Astronautical Congress', C4.6.2, Daejeon, Korea.(Oct.2009)

[5] Wang B, ***Yamaguchi T**, Hatai K, Komurasaki K, Arakawa Y, "HEATING STRUCTURE AND ITS SUSTAINING CONDITION OF LASER SUPPORTED DETONATION WAVE", '60th International Astronautical Congress', C4.6.3, Daejeon, Korea.(Oct.2009)

[6] ***Yamaguchi T**, Wang B, Shimada Y, Shimamura K, Hatai K, Komurasaki K, Arakawa Y, "Terminating Conditions of Laser Supported Detonation in Two Different Lasers", '6th International Symposium on Beamed Energy Propulsion', Scottsdale, Arizona, USA.(Nov.2009)

[7] ***Yamaguchi T**, Oda Y, Shimada Y, Shiraishi Y, Shibata T, Komurasaki K, Kajiwara K, Takahashi K, Kasugai A, Sakamoto K, Arakawa Y, "Visualization of Shock Wave Driven by Millimeter Wave Plasma in a Parabolic Thruster", '6th International Symposium on Beamed Energy Propulsion', Scottsdale, Arizona, USA.(Nov.2009)

国内学会での発表（自身で発表したもの．第一著者５件）

[8] ○山口敏和、畑井啓吾、小紫公也、荒川義博、「レーザー支持爆轟波におけるレーザー波長の影響」、『第 52 回宇宙科学技術連合講演会』、1I20、淡路島、2008 年 11 月

[9] ○山口敏和、畑井啓吾、小紫公也、荒川義博、「レーザー支持爆轟波内部の電子密度および電子温度の計測」、『日本航空宇宙学会第 40 期年会講演会』、B15、調布、2009 年 4 月

[10] ○山口敏和、小田靖久、白石裕也、梶原健、高橋幸司、春日井敦、坂本慶司、小紫公也、荒川義博、「マイクロ波推進におけるミリ波プラズマ生成初期の可視化」、『第 53 回宇宙科学技術連合講演会』、2K02、京都、2009 年 9 月

[11] ○山口敏和、小田靖久、梶原健、高橋幸司、春日井敦、小紫公也、坂本慶司、「大気圧ミリ波放電におけるプラズマ形状のビームプロファイルによる影響」、『プラズマ・核融合学会第 26 回年会講演会』、3aB06、京都、2009 年 12 月

[12] ○山口敏和、小田靖久、嶋田豊、小田章徳、澤原弘憲、嶋村耕平、梶原健、高橋幸司、坂本慶司、小紫公也、「ミラー系によるミリ波長距離伝送技術を用いたマイクロ波推進」、『平成 21 年度宇宙輸送シンポジウム』、STEP-2009-50、相模原、2010 年 1 月

国際会議発表（共著者４件）

[13] *Oda Y, Kajiwara K, Takahashi K, Kasugai A, Sakamoto K, **Yamaguchi T**, Shiraishi Y, Komurasaki K, "A study of shock wave supported by millimeter wave plasma in Microwave Rocket", '27th International Symposium on Space Technology and Science', 2009-b-47, Tsukuba, Japan.(Jul.2009)

[14] *Oda Y, **Yamaguchi T**, Kajiwara K, Takahashi K, Kasugai A, Komurasaki K, Sakamoto K, "Structure Formation of Atmospheric Millimeter Wave Breakdown on Non-Gaussian Beam", 'The 34th International Conference on Infrared, Millimeter, and Terahertz Waves', Busan, Korea.(Sep.2009)

[15] *Shimada Y, Shibata T, Oda Y, **Yamaguchi T**, Komurasaki K, Arakawa Y, Kajiwara K, Takahashi K, Kasugai A, Sakamoto K, "Propagating Structure of a Microwave Driven Shockwave Inside a Microwave Rocket", '6th International Symposium on Beamed Energy Propulsion', Scottsdale, Arizona, USA.(Nov.2009)

[16] *Wang B, **Yamaguchi T**, Hatai K, Komurasaki K, Arakawa Y, "Energy Absorption Structure of Laser Supported Detonation Wave", '6th International Symposium on Beamed Energy Propulsion', Scottsdale, Arizona, USA.(Nov.2009)

国内学会発表（共著者４件，うち１件は予定）

[17] ○白石裕也、山口敏和、小紫公也、小田靖久、梶原健、高橋幸司、春日井敦、坂本慶司、「前方吸気を想定したマイクロ波ロケットの部分充填率による推力最適化」、『平成 20 年度宇宙輸送シンポジウム』、No.60、相模原、2009年 1 月

[18] ○小田靖久、梶原健、高橋幸司、春日井敦、坂本慶司、山口敏和、白石裕也、小紫公也、「マイクロ波ロケットにおける PDE 型推力発生サイクル」、『デトネーションシンポジウム 2009』、筑波、2009 年 3 月

[19] 白石裕也、山口敏和、○小紫公也、小田靖久、梶原健、高橋幸司、春日井敦、坂本慶司、「マイクロ波電力および雰囲気圧力によるマイクロ波ロケットの推力最適化」、『第 49 回航空原動機・宇宙推進講演会』、A21、長崎、2009 年 3 月

[20] ○Wang Bin、嶋村耕平、山口敏和、小紫公也、荒川義博、「Experimental Investigation on the Shock Wave Generated by a Solid Laser Induced Plasma in Air」、『平成 21 年度衝撃波シンポジウム』、19-C-3-1、さいたま、2010 年 3 月（予定）